Massive Stars Near and Far
Proceedings IAU Symposium No. 361, 2024
J. Mackey, J. S. Vink, & N. St-Louis, eds.
doi:10.1017/S1743921322002952

Constraints on the stellar upper mass limit from simulations of UV disk ablation

N. Dylan Kee[1] and Rolf Kuiper[2]

[1]National Solar Observatory, 22 Ohi'a Ku St, Makawao, HI 96768, USA
email: dkee@nso.edu

[2]Faculty of Physics, University of Duisburg-Essen, Lotharstraße 1,
D-47057 Duisburg, Germany

Abstract. This contribution presents recent advances in identifying the stellar upper mass limit using simulations of UV radiative feedback during the star formation process. Generally, due to computational costs and a focus on au to parsec scales, simulations of massive star formation do not trace the flow of material to distances closer than a few au from the forming star. However, UV line-acceleration acts directly on accreting material in the sub-au circumstellar region, thereby efficiently ablating the surface layers off the protostellar disk. For stars on the order of a few hundred solar masses, this disk destruction rate exceeds the accretion rate, destroying the disk faster than it is replenished, and setting a maximum stellar mass as a function of metallicity that can be attained by single star formation channels.

Keywords. stars: formation, stars: mass function, stars: outflows, stars: early-type, stars: circumstellar matter

1. Introduction

One of the current major questions in the study of luminous massive stars concerns the stellar upper mass limit. While observations strongly suggest that such a limit exists, theory has thus far failed to conclusively identify either its physical origin or the actual value of this limit. However, it is clear that understanding this limit is crucially important due to the extreme impact of the most massive stars on their environments, the role these stars play as tracers of the structure and evolution of distant galaxies, and their place as the evolutionary precursors to exotic supernovae and high mass black holes.

In this contribution, we discuss recent work that constrains the upper mass limit of stars by examining the interplay of ultraviolet (UV) radiation with the circumstellar accretion disk at sub-au distances from forming massive stars (Kee et al. 2018, Kee and Kuiper 2019). By zooming in on this near-star region, we directly probe a volume that is normally omitted in studies of massive star formation due to the high computational cost of tracing accreting gas from the parsec-scale distances characteristic of a pre-stellar molecular cloud down to length scales on order the stellar radius of a zero-age main-sequence massive star. By examining this region, we capture critically important physics for setting the stellar upper mass limit also omitted by the current state-of-the-art simulations of massive star formation (e.g. Klassen et al. 2016, Kuiper and Hosokawa 2018, Tanaka et al. 2018, Mignon-Risse et al. 2021, Rosen 2022), namely the direct acceleration of material off of the accretion disk surface by stellar UV photons, and the associated disk mass loss. In the simulations presented here, we show that this disk mass-loss rate can exceed the accretion rate for stars with masses a few hundred times the mass of the Sun, thereby dispersing the inner disk faster than it can be replenished and preventing the star from growing to higher mass.

2. Description of the simulation suite

For this study, we set up a grid of simulations considering the innermost 20 stellar radii (R_*) around forming massive stars of a range of masses. As the crucial physics is the interaction of stellar UV photons with circumstellar disk material, we select stars with main-sequence-like radii for their mass and luminosity, namely stars which are hot enough to emit substantial UV photon fluxes. Based on computations of stellar structure in the presence of disk accretion by Hosokawa et al. (2010), the Kelvin-Helmholtz timescale becomes shorter than the accretion timescale around 20-30 $M_\odot$, fairly independent of the accretion rate. As such, we simulate stars of 25, 50, 75, and 100 $M_\odot$. For each stellar mass, we also consider a range of disk masses. By comparison with observations (see e.g. Beltrán and de Wit 2016; for a review) and prior simulations (e.g. Klassen et al. 2016, Tanaka et al. 2018, Oliva and Kuiper 2020, Rosen 2022), we extrapolate to the near-star conditions appropriate to disks of 10, 20, and 30 $M_\odot$ in 1000 au.

To describe the radiation force imparted on disk material through the interaction of UV photons with spectral lines of ionized metal species, we follow the Castor et al. (1975) formalism extended to be fully three-dimensional as discussed, for instance, in Kee et al. (2016). This extension to 3D is crucially important to the problem at hand, as the Castor et al. (1975) formalism focuses on the interaction of radially propagating photons with radially accelerating plasma. However, the finite angular size of the star allows photons to interact with non-radial acceleration, here the Keplerian shear of the circumstellar accretion disk, and thereby directly accelerate disk material away from the forming star.

3. Disk destruction rate

The most important property of the simulations carried out here is the rate at which material is stripped, or ablated, off the circumstellar disk, $\dot{M}_{\rm ab}$. To quantify this, we measure the rate at which material leaves the simulation volume through the outer boundary and subtract off the spherically symmetric wind mass-loss rate predicted for each stellar mass. The resulting disk destruction rate is plotted for all models in Figure 1.

Considering each panel alone, we see that the disk mass does not play an important role in setting the ablation rate. Specifically, the variation of ablation rate between simulations with the same star and different disks can be attributed to a time delay caused by the more massive disks taking longer to evacuate than the less massive disks. As such, more massive disks can be taken as a proxy for accretion more efficiently replenishing the disk and more effectively keeping the disk and star connected. Meanwhile, the tendency for ablation rate to increase at later times in simulations with less massive disks can be attributed to the radial falloff in disk density allowing less dense material to be exposed to the direct irradation from the star at later times in the simulation once the inner disk is eaten away. The one exception to this is the set of simulations with a 25 $M_\odot$ star, where the ablation rate is notably the lowest, and as such none of the simulations with a 25 $M_\odot$ star evacuate a substantial fraction of the circumstellar disk in one year.

This brings us to a second important take away from these simulations, namely that comparing the panels of Figure 1 shows an almost two order-of-magnitude spread in ablation rate from simulations with a 25 $M_\odot$ star and those with a 100 $M_\odot$ star. In order to examine this trend, it is natural to scale the ablation rates with the predicted spherically symmetric wind mass-loss rate predicted for each individual star. As we are interested in the case where the ablation rate is most akin to what it would be in the

https://doi.org/10.1017/S1743921322002952 Published online by Cambridge University Press

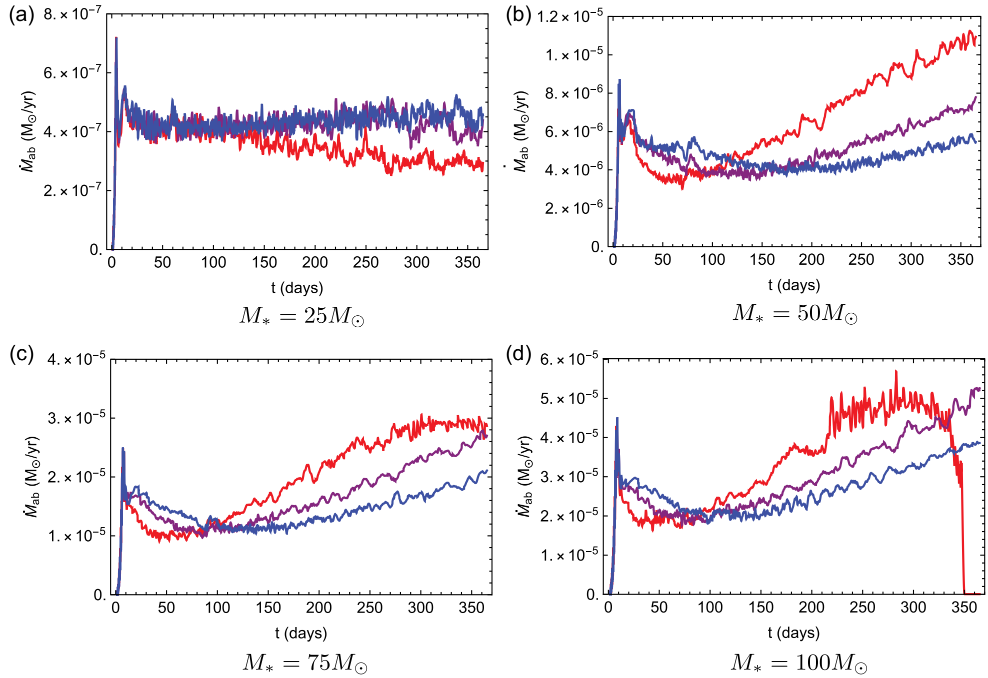

Figure 1. Disk destruction rate in solar masses per year for 25 (top, left), 50 (top, right), 75 (bottom, left), and 100 (bottom, right) solar mass stars. In each panel the three curves denote simulations with 10 (red), 20 (purple), and 30 (blue) $M_\odot$ disks. In the early simulation (the full simulation for the 25 $M_\odot$ star), the curves with the lowest, middle, and highest disk destruction rate are those with 10, 20, and 30 $M_\odot$ disks respectively. With the exception of the simulation with the 25 $M_\odot$ star, this ordering reverses as the simulation progresses.

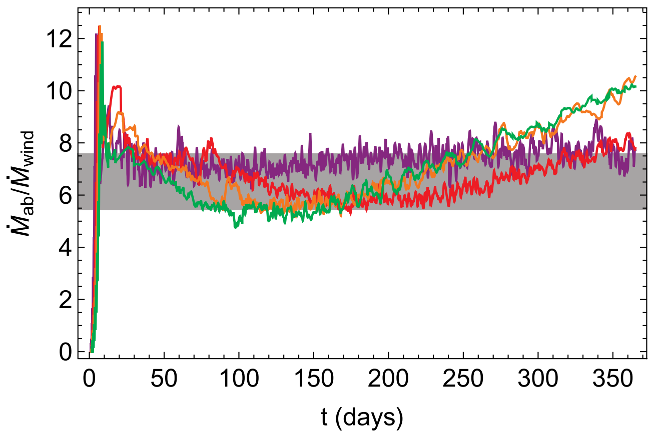

Figure 2. Disk destruction rate over spherically symmetric wind mass-loss rate for 25 (purple), 50 (red), 75 (orange), and 100 (green) solar mass stars. The grey bar at $\dot{M}_{\rm ab} = 6.5 \pm 1\ \dot{M}_{\rm wind}$ is put in by eye to draw attention to the overall uniformity of behavior between the simulations.

presence of accretion, we take the simulations with 30 $M_\odot$ disks, perform this rescaling, and plot the results in Figure 2. Immediately, it is evident that all simulations show disk evacuation at a rate $6 \sim 7$ times the wind mass-loss rate. Going forward this uniformity of behaviour, highlighted by the grey shading in Figure 2, allows us to analytically predict

https://doi.org/10.1017/S1743921322002952 Published online by Cambridge University Press

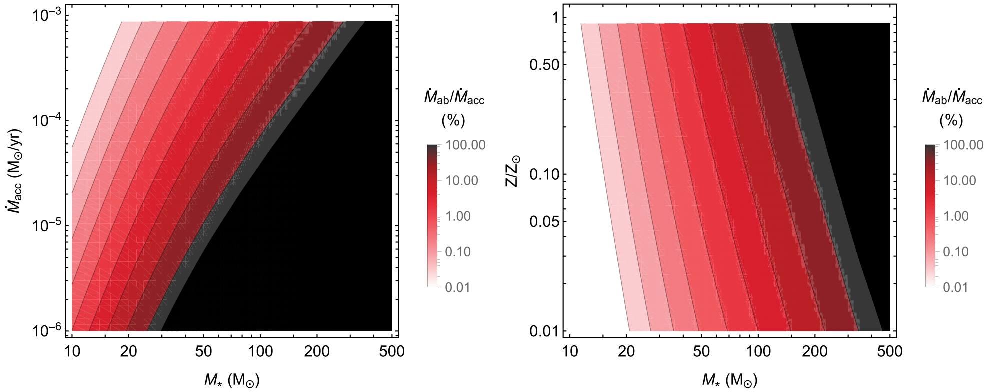

Figure 3. Ablation efficiency $\dot{M}_{\rm ab}/\dot{M}_{\rm acc}$ at Solar metallicity (left) and as a function of metallicity for an accretion rate of 10^{-4} $M_\odot$/yr (right). The black region on the right where $\dot{M}_{\rm ab} > \dot{M}_{\rm acc}$ denotes a forbidden region where stars can not form, such that the left edge of this region is the stellar upper mass limit as a function of accretion rate.

the rate at which forming massive stars can evacuate their disks simply by scaling the wind mass-loss rate up by a constant factor.

4. The stellar upper mass limit

With these results, we can now predict a stellar upper mass limit. To do so, we take the fully analytic Kudritzki et al. (1989) mass-loss rates computed for zero-age main-sequence stars using the mass-radius-luminosity relations taken from the Geneva stellar evolution code (Ekström et al. 2012, Yusof et al. 2013), boosted by the factor 6.5 found in the prior section. We then compare to a range of mass accretion rates $\dot{M}_{\rm acc}$ appropriate to forming massive stars, and compute the fraction of the accretion that would be removed from the disk by ablation. We plot a map of this 'ablation efficiency' at Solar metallicity in the left panel of Figure 3. The black region at the right of this figure is a forbidden region where $\dot{M}_{\rm ab} > \dot{M}_{\rm acc}$ and as such stars can not form. Therefore, for a chosen accretion rate the maximum mass of star that can form can be read off directly as the left edge of this forbidden region. Guided by observations and prior simulations, accretion rates for forming massive stars can reach $10^{-4} - 10^{-3} M_\odot$/yr, yielding an upper mass limit of a few hundred $M_\odot$, in good agreement with the most massive stars observed. Below this hard limit, it is important to note that order tens of percent of the accretion flow is already diverted for a star approximately half the maximum allowed mass, suggesting that ablation plays an important role in stellar feedback on the accretion disk even before the point where it alone can set the stellar upper mass limit.

Taking this one step further, we note that wind mass-loss rate, and as such ablation rate, is a function of metallicity Z, usually taken to be a power-law $\dot{M}_{\rm wind} \propto (Z/Z_\odot)^\alpha$. This means that ablation predicts a maximum allowed stellar mass also as a function of metallicity. To illustrate this, we take $\alpha = 0.5$ in the scaling relation above, and plot $\dot{M}_{\rm ab}/\dot{M}_{\rm acc}$ as a function of metallicity for a fixed accretion rate 10^{-4} $M_\odot$/yr (Figure 3, right). As would be predicted, a decrease of metallicity leads to decreases in both the available opacity for UV line-driving and the efficiency of ablation, and as such implies an increase in stellar upper mass-limit. This is again in good agreement with observations of star formation in the lower metallicity environments of the Magellanic Clouds.

https://doi.org/10.1017/S1743921322002952 Published online by Cambridge University Press

5. Implications and future directions

Given that ablation operates at a notably smaller scale than other forms of feedback from forming massive stars on their environments (e.g. radiation pressure on dust grains, MHD driven outflows, and photoionization), it is likely that there is minimal direct interaction of these larger scale feedback mechanisms with ablation beyond modifying the rate of accretion that ablation must contend with. As such, the stellar upper mass limits predicted here are robust, as they are provided as a function of the accretion rate that reaches the near-star ablation zone. Looking back outwards, the disk surface flows launched by ablation likely do impact feedback on larger scales as larger scale feedback can be expected to interact with the additional kinematic component of the disk wind. Additionally, these low-angle disk winds can also be expected to be observed as they proceed to these larger scales (see Maud et al. 2018; for a recent potential observation of ablation at these larger scales). Therefore, future work will focus on directly including ablation in larger scale simulations to provide observational predictions, to examine this interaction of larger scale feedback with the flows launched by ablation, and to better constrain the accretion rates that reach the ablation zone and therefore the single value of the stellar upper mass limit as a function of the star formation environment.

6. Appendix A. Questions

D. Baade: The ablation rate appears to be rising near the end of each simulation. Could one have learned more by running these simulations for a longer period of time?
N. D. Kee: This is an artifact of the simulation set up. Since these simulations did not include accretion from larger radii, this rise is the accelerating ejection of the disk as the disk is detached from the star. Therefore, while it would be desirable to run the simulations longer to determine the asymptotic ablation rate, this will have to wait for the inclusion of the associated disk replenishment physics.

D. Hendriks: What is the relation between the outflow per unit surface area and the location where the outflow happens? Specifically, does outflow per unit surface area increase with distance from the star or is it mostly in the inner disk?
N. D. Kee: The ablation rate per unit surface area increases most strongly in the inner disk, namely most of the ablation flow is directly accelerated at the nearest point in the disk to the star, and minimal additional disk material is entrained further away.

A. de Koter: Does photoevaporation also play a role in the disk dispersal?
N. D. Kee: Moving from very massive stars to later spectral types does lead to a transition as ablation becomes less strong and photoevaporation increases in efficiency. Similarly, Tanaka et al. (2018) showed that photoevaporation is a dominant effect at low metallicity, where once again ablation is weak. The details of where both of these transitions occur, and how the two transitions interplay with one another at sub-Solar metallicity is a fertile topic for future research.

J. Regan: Lionel Haemmerlé in his talk discussed accretion rates of $> 1 M_\odot$/yr. Could you comment on how your findings might influence the formation of supermassive stars?
N. D. Kee: Since supermassive stars are formed at low metallicity, this is likely a part of the parameter space where ablation plays a more minor role. Future work could confirm this by computing UV line-driven wind mass loss rates for supermassive stars.

S. Oey: Is ablation accounted for in models of other circumstellar disks, e.g., excretion disks of Oe/Be stars? Presumably that sets the life expectancy of such disks?
N. D. Kee: Yes, earlier work in the series of papers on which this talk was based did consider ablation in classical Oe/Be star disks (Kee et al. 2016). A major finding of this work was that ablation alone is compatible with the rate of disk destruction in Be stars, and the dearth of Oe stars at solar metallicity.

References

Beltrán, M. T. & de Wit, W. J. 2016, Accretion disks in luminous young stellar objects. *A&AR*, 24, 6.

Castor, J. I., Abbott, D. C., & Klein, R. I. 1975, Radiation-driven winds in Of stars. *ApJ*, 195, 157–174.

Ekström, S., Georgy, C., Eggenberger, P., Meynet, G., Mowlavi, N., Wyttenbach, A., Granada, A., Decressin, T., Hirschi, R., Frischknecht, U., Charbonnel, C., & Maeder, A. 2012, Grids of stellar models with rotation. I. Models from 0.8 to 120 $M_\odot$ at solar metallicity (Z = 0.014). *A&A*, 537, A146.

Hosokawa, T., Yorke, H. W., & Omukai, K. 2010, Evolution of Massive Protostars Via Disk Accretion. *ApJ*, 721(1), 478–492.

Kee, N. D. & Kuiper, R. 2019, Line-driven ablation of circumstellar discs: IV. The role of disc ablation in massive star formation and its contribution to the stellar upper mass limit. *MNRAS*, 483(4), 4893–4900.

Kee, N. D., Owocki, S., & Kuiper, R. 2018, Line-driven ablation of circumstellar discs - III. Accounting for and analysing the effects of continuum optical depth. *MNRAS*, 479(4), 4633–4641.

Kee, N. D., Owocki, S., & Sundqvist, J. O. 2016, Line-driven ablation of circumstellar discs - I. Optically thin decretion discs of classical Oe/Be stars. *MNRAS*, 458(3), 2323–2335.

Klassen, M., Pudritz, R. E., Kuiper, R., Peters, T., & Banerjee, R. 2016, Simulating the Formation of Massive Protostars. I. Radiative Feedback and Accretion Disks. *ApJ*, 823(1), 28.

Kudritzki, R. P., Pauldrach, A., Puls, J., & Abbott, D. C. 1989, Radiation-driven winds of hot stars. VI. Analytical solutions for wind models including the finite cone angle effect. *A&A*, 219, 205–218.

Kuiper, R. & Hosokawa, T. 2018, First hydrodynamics simulations of radiation forces and photoionization feedback in massive star formation. *A&A*, 616, A101.

Maud, L. T., Cesaroni, R., Kumar, M. S. N., van der Tak, F. F. S., Allen, V., Hoare, M. G., Klaassen, P. D., Harsono, D., Hogerheijde, M. R., Sánchez-Monge, Á., Schilke, P., Ahmadi, A., Beltrán, M. T., Beuther, H., Csengeri, T., Etoka, S., Fuller, G., Galván-Madrid, R., Goddi, C., Henning, T., Johnston, K. G., Kuiper, R., Lumsden, S., Moscadelli, L., Mottram, J. C., Peters, T., Rivilla, V. M., Testi, L., Vig, S., de Wit, W. J., & Zinnecker, H. 2018, Chasing discs around O-type (proto)stars. ALMA evidence for an SiO disc and disc wind from G17.64+0.16. *A&A*, 620, A31.

Mignon-Risse, R., González, M., & Commerçon, B. 2021, Collapse of turbulent massive cores with ambipolar diffusion and hybrid radiative transfer. II. Outflows. *A&A*, 656, A85.

Oliva, G. A. & Kuiper, R. 2020, Modeling disk fragmentation and multiplicity in massive star formation. *A&A*, 644, A41.

Rosen, A. L. 2022, A Massive Star is Born: How Feedback from Stellar Winds, Radiation Pressure, and Collimated Outflows Limits Accretion onto Massive Stars. *arXiv e-prints*,, arXiv:2204.09700.

Tanaka, K. E. I., Tan, J. C., Zhang, Y., & Hosokawa, T. 2018, The Impact of Feedback in Massive Star Formation. II. Lower Star Formation Efficiency at Lower Metallicity. *ApJ*, 861(1), 68.

Yusof, N., Hirschi, R., Meynet, G., Crowther, P. A., Ekström, S., Frischknecht, U., Georgy, C., Abu Kassim, H., & Schnurr, O. 2013, Evolution and fate of very massive stars. *MNRAS*, 433(2), 1114–1132.